Arabian Journal for Science and Engineering (2018) 43:6413–6428
https://doi.org/10.1007/s13369-018-3183-5

RESEARCH ARTICLE - PETROLEUM ENGINEERING

Microstructure Behavior of Fly Ash-Based Geopolymer Cement Exposed to Acidic Environment for Oil Well Cementing

Syahrir Ridha[1] · Afif Izwan Abd Hamid[1] · Riau Andriana Setiawan[1] · Mohamad Arif Ibrahim[1] · Ahmad Radzi Shahari[1]

Received: 1 October 2017 / Accepted: 4 February 2018 / Published online: 23 March 2018

Abstract
Acidizing is a widely used technique to stimulate an oil well in order to enhance its production. When portland cement is placed in contact with acid fluids, it will dissolve and, at some time, will be fully degraded because the acids have reacted with calcium silicate hydrate which resulted in the breaking up of the cement intergranular structure. This in turn will give rise to well integrity issue. Instead of introducing a new acid type, which may not be as effective toward reservoir formation, researchers have come up with a new cementing material, namely geopolymer cement. Literature has shown that geopolymer cement is unreactive toward conventional acids. In addition, its strength may be improved by introducing Nano-silica in the admixture. However, the studies were conducted at ambient condition. The objective of this work is to investigate geopolymerization mechanism and microstructure behavior of fly ash-based geopolymer cement with Nano-silica admixture. Two cement slurries, geopolymer and Class G OPC, were prepared in accordance with API RP-10B. The slurries were cured for 24 h at 130 °C and 20.69 MPa at the HPHT curing chamber before being exposed to 15 wt% acid solution for 14 days. The reaction mechanism of the cement samples was investigated by using FTIR and XRD analyses. The results were further validated by carrying out SEM and EDS tests to evaluate the microstructure behavior and chemical compositions of the cured samples. Results show that fly ash-based geopolymer cement with 1 wt% of Nano-silica additive was the least affected cement samples after acid treatment as compared to a similar weight of Class G OPC.

Keywords Geopolymer · Fly ash · Nano-silica · Oil well cement · Microstructures · Acid

1 Introduction

Structural integrity is at the heart of every wellbore architectural design in oil and gas industry. In order to achieve maximum wellbore integrity in oil well, cement plays a key role [1]. In a wellbore, cement is used to provide zonal isolation and helps confer protection to casing against corrosive fluids [2]. Cement is also used as a binding element to permanently seal annular spaces between borehole wall and casing wall in which the cement sheath must prevent any fluid circulation between different rock layers [2]. A successful well cementing can enhance the wellbore integrity and thus will confirm the long-term well life. Recently, researchers had developed geopolymer cement to replace ordinary portland cement (OPC). This is due to the fact that OPC is highly reactive to conventional acids used in the industry and will, at some time, be fully degraded. A study by [3] reported that acid can penetrate OPC easily as 50% of the cement system is carbonate which is reactive to acid. Acid has reacted with calcium silicate hydrate which resulted in the breaking up of intergranular structure of the cement. Thus, it affected the microstructure and properties of the OPC, causing the zonal isolation to become ineffective [3].

OPC mainly consists of tricalcium and dicalcium silicates (C_3S and C_2S), which react with water to form calcium

✉ Afif Izwan Abd Hamid
afif_g03455@utp.edu.my

Syahrir Ridha
syahrir.ridha@utp.edu.my

Riau Andriana Setiawan
riau.andriana_g03436@utp.edu.my

Mohamad Arif Ibrahim
mohamad.arif_g03640@utp.edu.my

Ahmad Radzi Shahari
ahmadradzi.shahari@utp.edu.my

[1] Petroleum Engineering Department, Universiti Teknologi Petronas, Bandar Seri Iskandar, Perak, Malaysia

silicate hydrate (C–S–H) and portlandite or calcium hydroxide ($Ca(OH)_2$). OPC is highly alkaline, having pH above 12.5, and easily attacked by acid solutions. When OPC is attacked by sulfuric acid, the pH of the solution decreases. This reaction led to the formation of gypsum ($CaSO_4 2H_2O$) and ettringite ($3CaO{\cdot}Al_2O_3 3CaSO_4 31H_2O$) which were the main reason for the deterioration of OPC mortar [4]. One of the examples of OPC cement that is extensively being used for cementing oil and gas wells is API Class G cement [5]. API Class G cement is used as a basic well cement from surface to 8000 ft (2440 m) depth and can be used with accelerators and retarders to cover a wide range of well depths and temperatures [5].

The recent rise in the environmental degradation has become a concern to researchers as the production of API Class G cement had released tonnes of CO_2 into the environment [6]. As a result, researchers developed the alkali-activated cement by using industrial by-products, such as fly ash [6]. Between the year 2011 and 2012, the worldwide production of fly ash was approximately 780 Mt tonnes, making the application of alkali-activated geopolymer concrete by using fly ash an important area of research [7]. Geopolymer cement is low in calcium, alkali-activated aluminosilicate cement, which has gone through geopolymerization process that posed a high strength, with good volume durability, stability and resistance to acids [3,7]. Geopolymer cement had undergone chemical process where aluminosilicates had reacted with aqueous alkaline solution to produce a new class of inorganic binders [8,9]. This polymerization process involved a substantially fast chemical reaction which resulted in a three-dimensional polymeric chain reaction consisting of SiO_4 and AlO_4 linked alternately by sharing oxygen [3,5,8,10,11]. Alkaline solution is used to react with Si and Al to produce geopolymer binders. The most commonly used alkaline solution is sodium hydroxide (NaOH) and sodium silicate (Na_2SiO_3), which act as alkaline activators [3,9].

The setting and hardening mechanisms of the geopolymer material were studied by Davidovits [13]. This study mentioned that geopolymer cement gained its strength through the reaction between aluminosilicate oxides with alkali polysilicates, producing Si–O–Al bonds with a (Si_2O_5, Al_2O_2) n chain. This bond is accomplished by calcining aluminosilicate hydroxides (Si_2O, $Al_2(OH)_4$) or by the condensation of SiO and Al_2O vapors along with the production of condensed silica fume ($2SiO_2$) and corundum (Al_2O_3) [13]. Hence, the key difference in setting and hardening of OPC mortar and geopolymer cement lies in their chemical structure and activation mechanism [14].

There were several studies that focused on strengthening the bonding structure of produced cement system by including pozzolanic materials, such as Nano-silica, to enhance the resistance of the cement paste from acid attack [9,11–14]. A study by Santra et al. [16] described the inclusion of nanoscale particles into portland cement paste mortar or concrete can impart functionality into cement, yielding a variety of different emergent property enhancements which include early strength development, increased long-term tensile-to-compressive strength ratio, viscosity enhancement and total increase in the early-stage compressive strength. Investigation into the reaction mechanism and microstructure behavior of geopolymer cement, incorporating Nano-silica with respect to acid exposure, however, remains limited. This paper aims to study the degradation process of geopolymer cement due to hydrochloric and sulfuric acid attack, including the microstructure.

2 Materials and Methods

2.1 Materials

The main materials for this research are fly ash (Class C), API (American Petroleum Institute) Class G cement, Nano-silica, sodium hydroxide (NaOH), sodium silicate (Na_2SiO_3), distilled water, hydrochloric acid and sulfuric acid. The chemical composition of fly ash and API Class G cement, as obtained from X-ray fluorescence (XRF) analysis, is shown in Tables 1 and 2, respectively.

Table 1 Composition of Class C fly ash cement

	Fly ash
SiO_2 (%)	32.44
Al_2O_3 (%)	12.22
Fe_2O_3 (%)	23.58
CaO (%)	20.66
MgO (%)	2.35
SO_3 (%)	2.40
Na_2O (%)	0.87
Rem. (%)	5.48

Table 2 Composition of API Class G cement

	API Class G
SiO_2 (%)	8.70
Al_2O_3 (%)	1.81
Fe_2O_3 (%)	–
CaO (%)	74.4
MgO (%)	–
SO_3 (%)	–
Na_2O (%)	–
Rem. (%)	15.09

2.2 Methods

Alkaline solution was prepared by mixing 8 M of sodium hydroxide and 97 wt. % of sodium silicates with a ratio of 1:2.5 in a 1-L Erlenmeyer flask, while fly ash and Nano-silica (1, 2 and 3% by weight of fly ash) were premixed in a dry beaker. Initially, alkaline solution was poured into Waring M3080 constant speed mixer. This initial solution was mixed at 4000 rpm for 15 s. Fly ash with Nano-silica (0, 1, 2, 3% by weight of fly ash) was then poured into the mixer and mixing was continued at 12,000 rpm for another 35 s. 0.44% by weight of cement (BWOC) alkaline activator to cement ratio was used for every cement slurry to achieve the highest compressive strength, as was reported by Ridha and Yerikania [12].

A similar procedure was carried out during the Class G OPC mixing while replacing alkaline solution with distilled water. All cement slurries were prepared in accordance with API RP-10A and API RP-10B-2 [16,17]. Once the cement slurries were well mixed, it was poured into a 5 cm cubic mold and was cured in a high-pressure–high-temperature (HPHT) curing chamber at 20.69 MPa and 130 °C for 24 h. A detailed composition of the cement recipe is provided in Table 3. Commercial grade 37% hydrochloric acid and 96% sulfuric acid by mass were diluted to 15% of mass by using distilled water. The 15 wt% concentration of the acid used in this research is according to Halliburton practice for acid pre-flush stage [18,19]. The diluting process was done inside a fume hood. Then, the cement cube samples were exposed to the acidic environment inside a water bath for 14 days at 65 °C, which is the average temperature inside Malaysian oil well [12].

Compressed strength of the cement samples before and after acid exposure was investigated by using ELE ADR 3000 with a capacity of 3,000 kN in the cubical samples. The compressive strength test was measured according to ASTM C 109 [21]. FTIR was performed on the samples by using a Perkin Elmer spectrum One/BX spectrometer that has a wave range of 7800–350 cm^{-1} and the KBr pellet technique, where 3 mg powder sample was mixed with 100 mg KBr. XRD analysis was done by using Pananalytical XPERT3 powder diffractometer of scanning range at 5–65 (2θ) per min and time steps of 0.05 (2θ).

SEM analysis was done by using FESEM (SUPRA 55VP, Germany) to analyze the microstructure behavior of cement samples. Cement cubes were cut into half by using core trimmer and cutoff machine. The samples were taken from the affected surface (1–2 mm) after acid exposure, and analysis was done by observing the affected area at 400 X magnification. EDS analysis was done by using AztecEnergy EDS microanalysis software to characterize the material composition of samples inside SEM. Types of cement samples and their acid environment are provided in Table 4.

Table 3 Composition of cement samples

Samples	Cement (600g)		
	Class G	Fly ash (%)	Nano-Silica (%)
OPC[a]	100	–	–
GC[b]	–	100	–
NG1[c]	–	99	1
NG2[d]	–	98	2
NG3[e]		97	3

[a]API Class G cement
[b]Pure geopolymer cement
[c]Geopolymer cement with 1 wt% Nano-silica additive
[d]Geopolymer cement with 2 wt% Nano-silica additive
[e]Geopolymer cement with 3 wt% Nano-silica additive

Table 4 Types of cement and their acid environment

Types of sample	Description	
	Types of cement	Acid environment
OPC_B	API Class G	–
OPC_H		15% HCl
OPC_S		15% H_2SO_4
GC_B	Pure geopolymer cement	–
GC_H		15% HCl
GC_S		15% H_2SO_4
NG1_B	Geopolymer cement with 1 wt% Nano-silica	–
NG1_H		15% HCl
NG1_S		15% H_2SO_4
NG2_B	Geopolymer cement with 2 wt% Nano-silica	–
NG2_H		15% HCl
NG2_S		15% H_2SO_4
NG3_B	Geopolymer cement with 3 wt% Nano-silica	–
NG3_H		15% HCl
NG3_S		15% H_2SO_4

3 Results and Discussion

3.1 Mechanical Property of Geopolymer and Class G Cement

3.1.1 Compressive Strength

Figure 1 shows the compressive strength result of samples before and after being exposed to hydrochloric and sulfuric acid solutions. It was shown that before acid exposure, NG1_B produced the highest strength as compared to

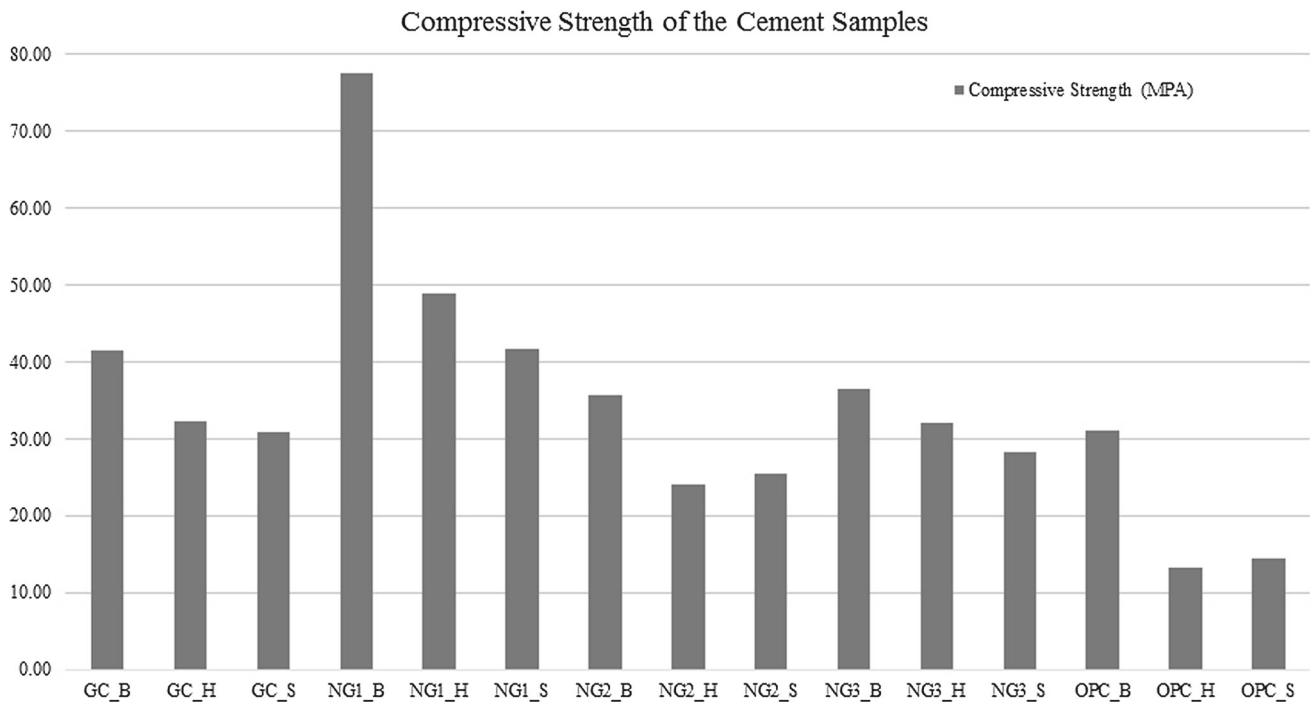

Fig. 1 Compressive strength result for the cement samples before and after exposed to acidic environment

OPC_B, GC_B, NG2_B and NG3_B, which is 77.60 MPa. NG1_B showed the workability of the pozzolanic material Nano-silica that enhances the strength of the geopolymer cement by filling up the spaces between gel formed by geopolymerization process due to its small size. Thus, this process led to a more compact cement structure. Addition of Nano-silica beyond 1 wt% caused the geopolymer to suffer strength reduction. This finding is in agreement with Ridha et al. [12] who mentioned that the optimal amount of Nano-silica is 1 wt%, which is necessary to consider the threshold of nano-material contents to enhance hydrated cement paste properties by pozzolanic reaction. Such result can be explained that geopolymer with high Nano-silica content had suffered flocculation, as Nano-silica did not disperse thoroughly into the cement system.

Figure 1 also shows that the cement samples strength had degraded after being exposed to acid treatment. It showed that hydrochloric and sulfuric acids manage to penetrate the cement samples, reacted with the elements inside them and causing them to degrade in strength. However, after being exposed to both acid environments, the strength of NG1 samples was still higher than the value of pure geopolymer cement before acid exposure, GC_B. Although geopolymer cements suffer strength reduction after the test, the strength was still higher than Class G as the samples possess a lower strength after being exposed to acid, which was 1925 psi and 2086 psi for OPC_H and OPC_S, respectively.

Based on recorded data, the compressive strength was adequate for most cementing operations, which was 500 psi [22]. Thus, geopolymer offers a greater strength as compared to the conventional Class G cement.

3.2 Reaction Mechanism Behavior of Geopolymer and Class G Cement

3.2.1 FTIR Analysis

The purpose of running FTIR analysis is to investigate the vibrational transitions and rigidity of chemical bonds present in the cement samples. By conducting FTIR, changes in chemical bonds and spectrum upon the alkali activation process can be identified, and the effects of Nano-silica toward geopolymer cement system can be investigated by searching the major reaction zones of Si–O and Al–O [6]. In FTIR analysis, the higher the wavenumbers, the higher the energy needed to form those bonds, thus causing it to be reactive, unstable and weak. This study analyzes the wavenumbers of the cement samples within the range of 4000–400 cm^{-1}. In geopolymer materials, the identification of IR spectral bands was performed according to the study by Bakharev [23]. The strongest vibration at 960 cm^{-1} was assigned to asymmetrical Al–O–Si stretch. The next strongest bands of 1600–1650 cm^{-1} and 3300–3380 cm^{-1} were assigned to the symmetric stretching bands of O–H and H–O–H, respectively.

Figures 2, 3, 4 and 5 show the IR spectra of the geopolymer cement before and after immersion test with hydrochloric acid and sulfuric acid solutions. All geopolymer cement samples exhibit the same behavior for this test. The symmetric

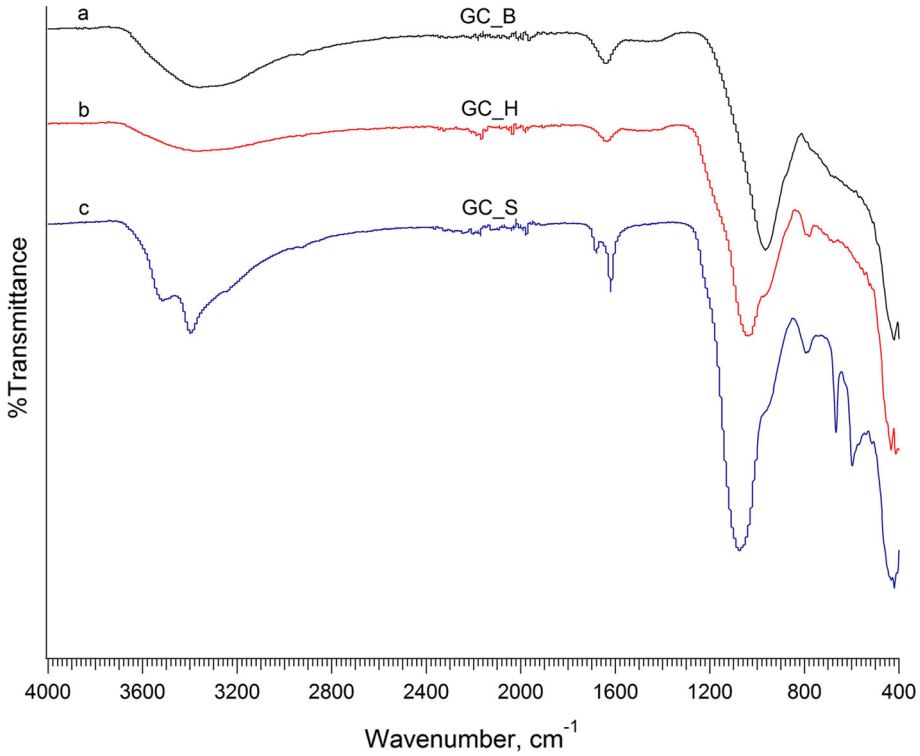

Fig. 2 IR spectra of GC samples **a** before test, **b** exposed to 15 wt% hydrochloric acid solution for 14 days, and **c** exposed to 15 wt% sulfuric acid solution for 14 days

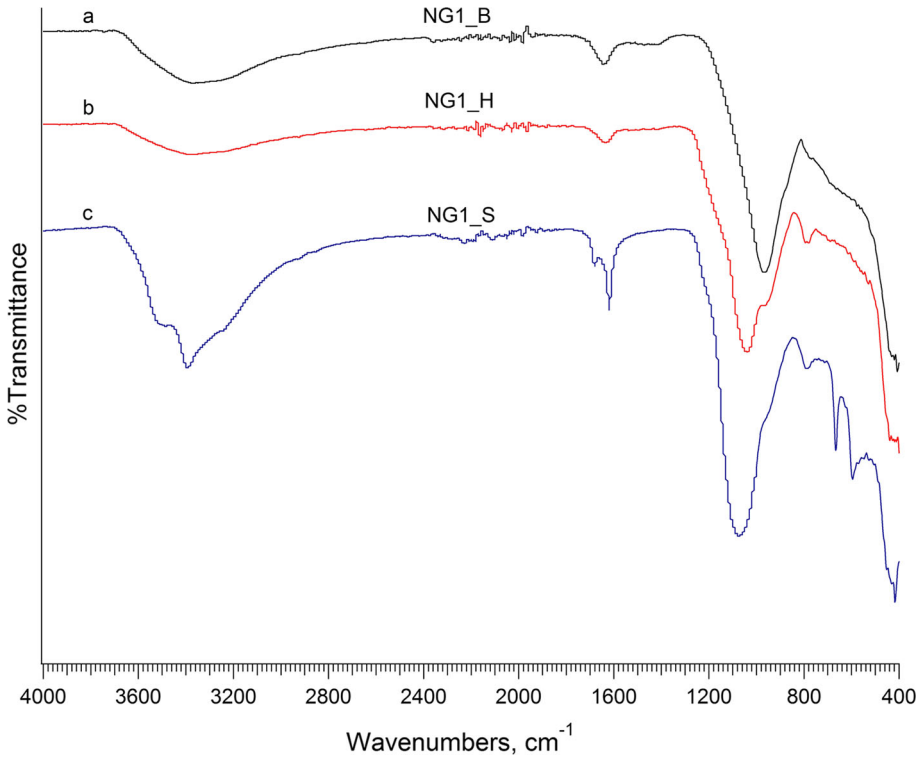

Fig. 3 IR spectra of NG1 samples **a** before test, **b** exposed to 15 wt. % hydrochloric acid solution for 14 days, and **c** exposed to 15 wt. % sulfuric acid solution for 14 days

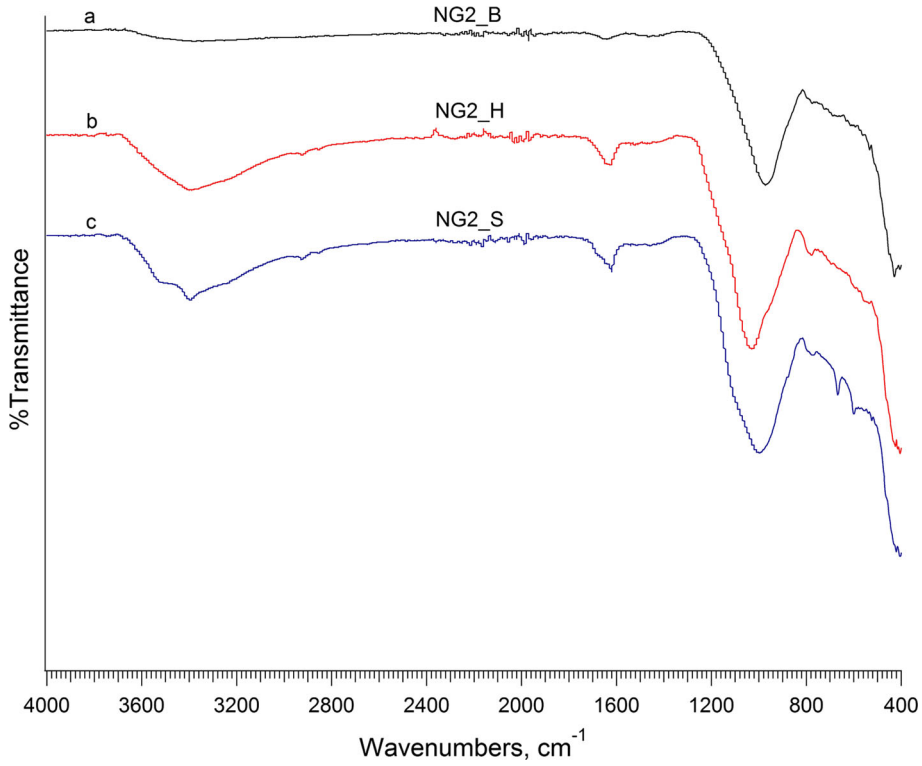

Fig. 4 IR spectra of NG2 samples **a** before test, **b** exposed to 15 wt% hydrochloric acid solution for 14 days, and **c** exposed to 15 wt% sulfuric acid solution for 14 days

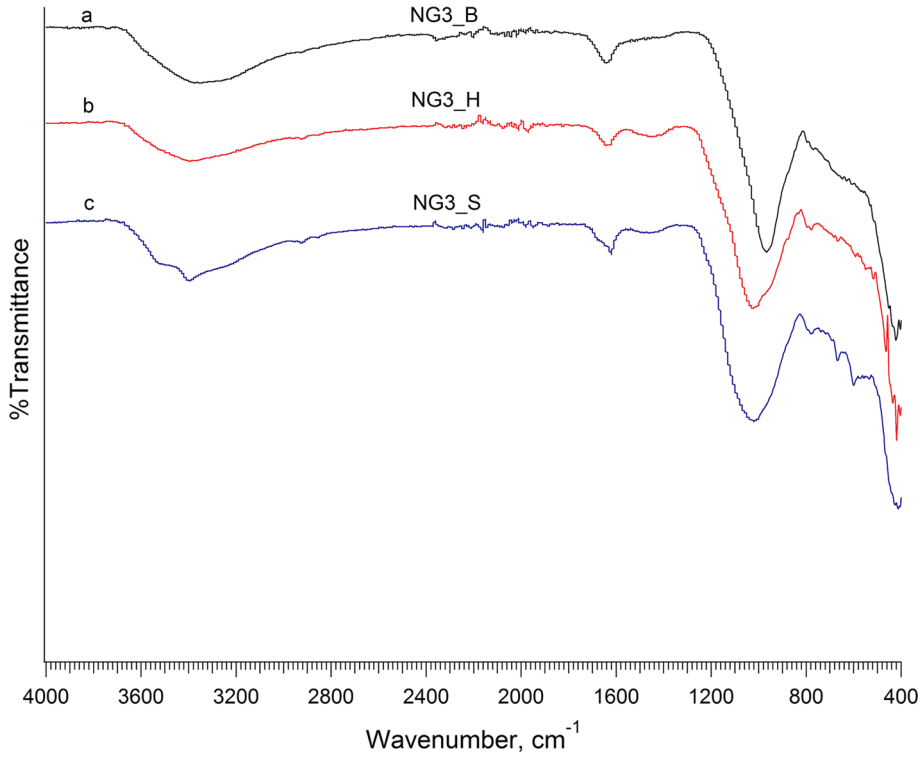

Fig. 5 IR spectra of NG3 samples **a** before test, **b** exposed to 15 wt% hydrochloric acid solution for 14 days, and **c** exposed to 15 wt% sulfuric acid solution for 14 days

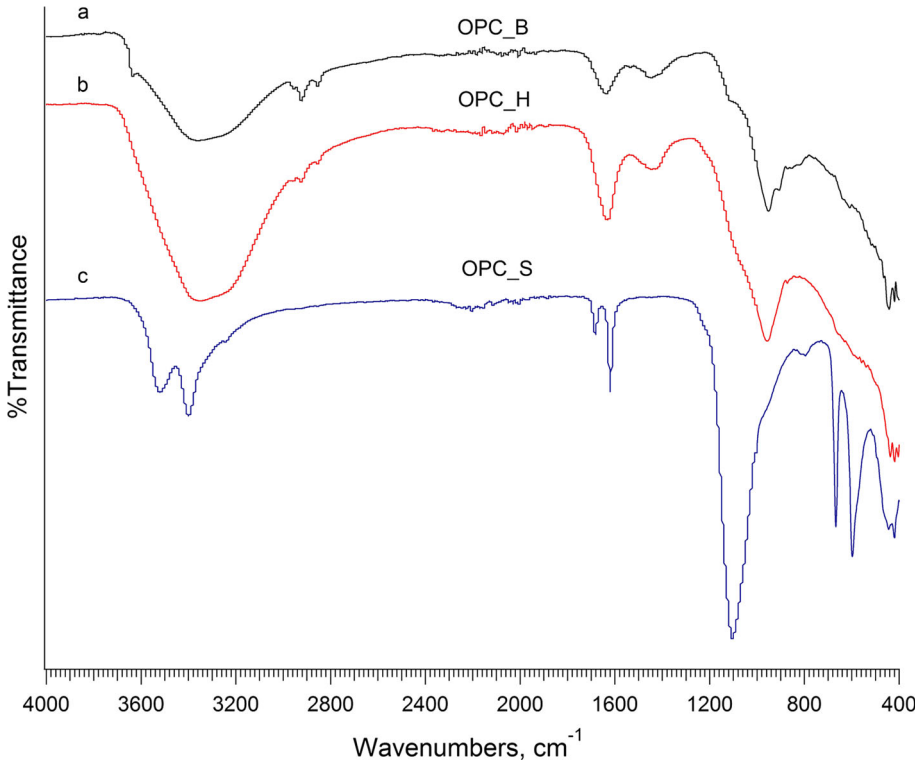

Fig. 6 IR spectra of OPC samples **a** before test, **b** exposed to 15 wt% hydrochloric acid solution for 14 days, and **c** exposed to 15 wt% sulfuric acid solution for 14 days

Si–O–Si stretching bands were detected in all unexposed cement samples, GC_B (Fig. 2a), NG1_B (Fig. 3a), NG2_B (Fig. 4a) and NG3_B (Fig. 5a) at 960 cm^{-1}. These profiles indicated that the geopolymerization of NaOH and activated fly ash has taken place at this region and Si/Al ratio in polymer has increased, in which N–A–S–H gels are formed and contributed to the increase in strength.

After acid exposure, the wavenumbers of these samples shift from 960 cm^{-1} to a higher frequency, as seen in Figs. 2, 3, 4 and 5. The shift in wavenumbers indicated that the cement samples after acid exposure had decelerated geopolymerization process, thus affecting the geopolymer cement structure and influencing the compressive strength as indicated in Fig. 1. Water component was detected at 1600–1650 cm^{-1} and at a broad region of 3300–3380 cm^{-1} for all unexposed geopolymer cement samples. The vibrations for these two regions (1600–1650 cm^{-1} and 3350–3400 cm^{-1}) showed some differences after being exposed to acid. After the hydrochloric acid environment exposure, the behavior of cement samples GC_H (Fig. 2b) and NG1_H (Fig. 3b) was similar to the samples before exposure, except at the broad region where NG2_H (Fig. 4b) and NG3_H (Fig. 5b) shifted to a slightly higher frequency to 3400 cm^{-1}. The presence of gypsum was detected in every geopolymer cement sample after acid exposure indicated by wavenumber 1620 cm^{-1}. Meanwhile, asymmetrical bands were detected at the broad region for all samples in the sulfuric acid test. This phenomenon indicated that the bond had become weaker as more energy was needed to form the bond. Overall, there were significant shifts in IR spectral bands of all geopolymer samples exposed in sulfuric acid solution, indicating that as compared to hydrochloric acid, sulfuric acid is more reactive toward geopolymer cement, causing the extensive dealumination and depolymerization. This analysis explained as to why geopolymer cements exposed to sulfuric acid experienced severe compressive strength degradation as compared to exposure to hydrochloric acid.

The IR spectra for Class G cement are shown in Fig. 6. The identification of the IR spectral bands for Class G cement is in accordance with the study by Hughes et al. [24]. The strongest vibration at 900–1000 cm^{-1} was assigned to C_3S or C_2S Si–O stretching. The next band located at 1600–1650 cm^{-1} was assigned to the presence of gypsum. The band located at 2850–2950 cm^{-1} was assigned to calcium carbonate. The stretching of O–H was located at 3300–3400 cm^{-1}, and the presence of calcium hydroxide (CaOH) was located at 3600–3650 cm^{-1}.

Similar to geopolymer cement, Class G cement also demonstrated a shift in IR wavenumbers after acid exposure. Both OPC_H (Fig. 6b) and OPC_S (Fig. 6c) symmetric stretching of Si–O shift from 900–950 cm^{-1} to a higher frequency which led to a weaker bond as more energy was needed for them to form. OPC_H shifted to 960 cm^{-1}, while OPC_S shifted further to 1100 cm^{-1}. In addition, OPC_H and OPC_S also detected the presence of calcium chloride and gypsum, respectively, in the cement samples at 1600–

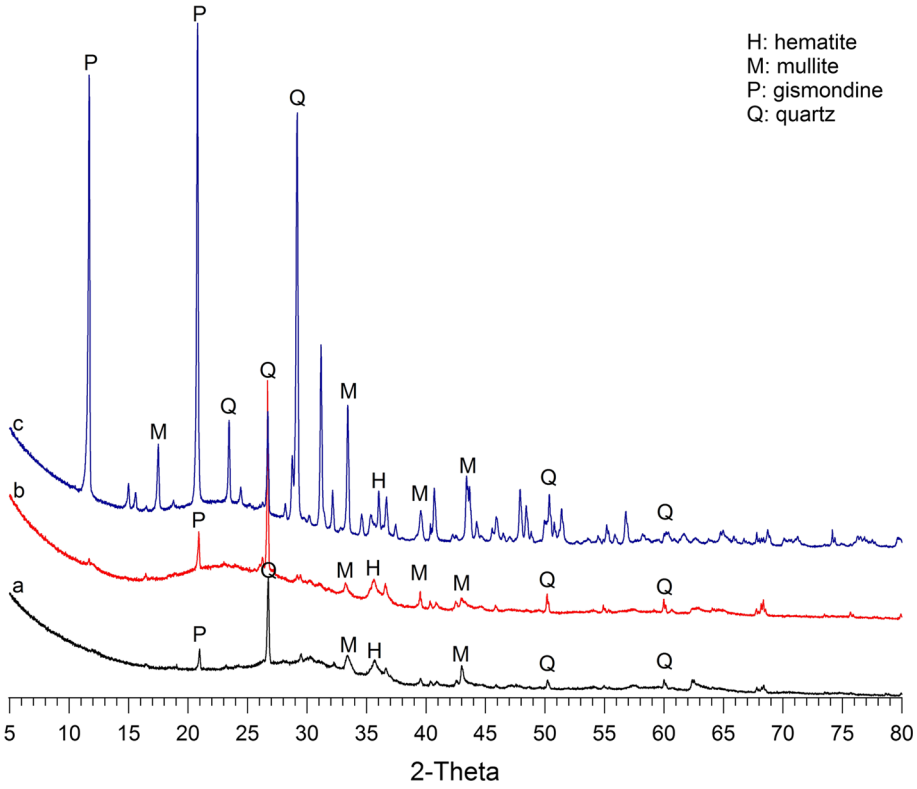

Fig. 7 XRD of GC samples **a** before test, **b** exposed to 15 wt% hydrochloric acid solution for 14 days, and **c** exposed to 15 wt% sulfuric acid solution for 14 days

1650 cm^{-1} region, and that only OPC_S had used more energy due to the presence of asymmetric stretching band located at 1680 cm^{-1}wavenumber. Thus, the presence of calcium chloride and gypsum had caused the cement samples to degrade in strength. Calcium hydroxide which is the main ingredient in Class G cement was initially detected at 3640 cm^{-1}. Calcium hydroxide in the cement systems had reacted with the hydrochloric acid and sulfuric acid and produced salts known as calcium chloride and calcium sulfate, respectively. This reaction phenomenon explains the extreme strength degradation in Class G cement after acid exposure. Furthermore, OPC_S also showed symmetric and asymmetric stretching bands at 3400 and 3520 cm^{-1}, respectively, which indicated the presence of sulfate minerals of either gypsum, bassanite, syngenite or anhydrite, which can be confirmed by using the XRD test.

3.2.2 XRD Analysis

Figures 7, 8, 9 and 10 show XRD spectra of the geopolymer cement before and after being exposed to 15 wt. % hydrochloric acid and sulfuric acid solution for 14 days. Traces of quartz, gismondine, mullite and hematite were detected in the XRD spectrum before and after the test. It was shown that the major XRD peaks corresponded to gismondine (P) and quartz (Q). The presence of gismondine ($CaAl_2Si_2O_8{\cdot}4H_2O$), a hydrated aluminosilicate mineral in the cement system, showed that geopolymer cement had hydrated and gained in strength when exposed to 65 °C temperature. However, its effectiveness needs to be measured by using a different approach. Figure 7 shows that there was no significant change after the sample was exposed to hydrochloric acid. When the diffraction pattern was minutely examined, it was noticed that intensity and sharpness of the diffraction peak at around 27° increased as compared to the sample before acid exposure. In this case, increase in sharpness of the diffraction peaks may be due to the increase in the activation energy as the acid solution had reacted with minerals inside the cement system. It is interesting to note that after the sample was exposed to sulfuric acid environment some new peaks appeared. These new and sharper diffraction peaks represented the minerals gismondine and quartz. These indicated that more energy was used when the sample was exposed to sulfuric acid as compared to hydrochloric acid.

Meanwhile, the effect of adding Nano-silica to the cement system is shown in Figs. 8, 9 and 10. Generally, the diffraction peaks representing gismondine and quartz minerals detected in the cement system were more as compared to pure geopolymer cement in Fig. 7. The effect of adding 1 wt. % Nano-silica into the geopolymer cement is shown in Fig. 8. The XRD profile before acid exposure for this sample showed that the quartz peaks were sharper than the sample in Fig. 7. It indicated the effectiveness of Nano-silica in

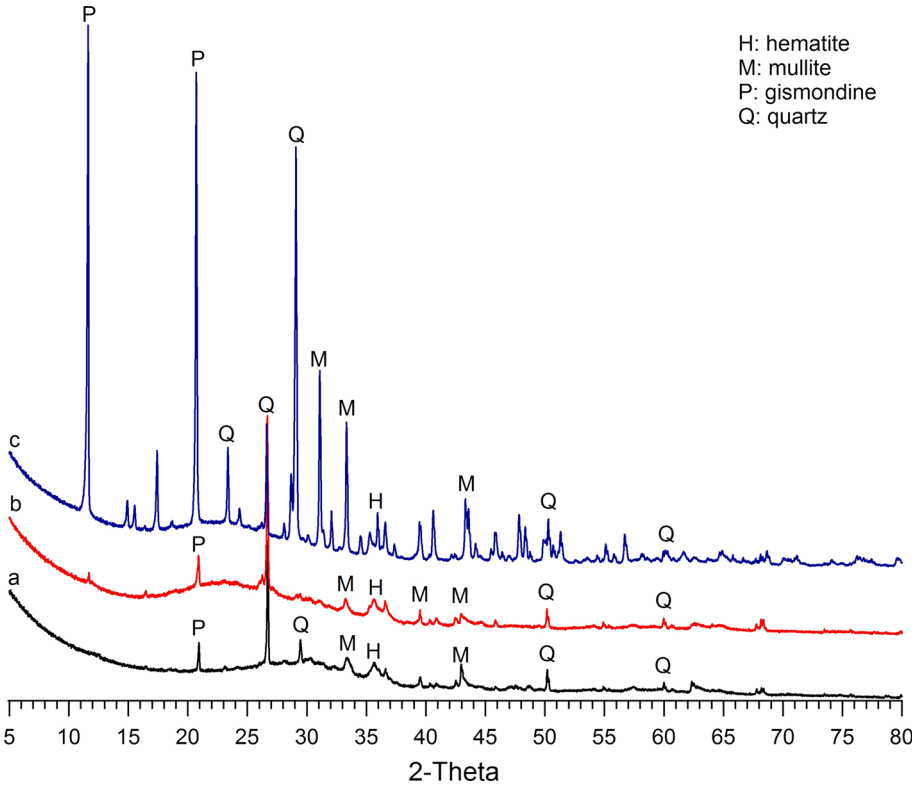

Fig. 8 XRD of NG1 samples **a** before test, **b** exposed to 15 wt% hydrochloric acid solution for 14 days, and **c** exposed to 15 wt% sulfuric acid solution for 14 days

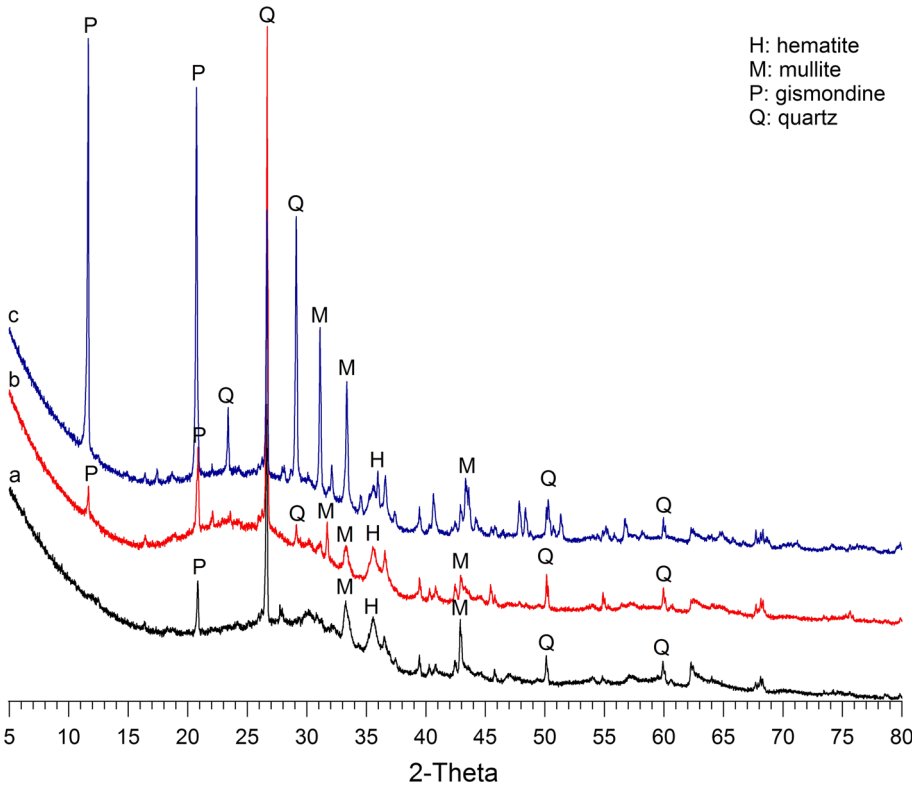

Fig. 9 XRD of NG2 samples **a** before test, **b** exposed to 15 wt% hydrochloric acid solution for 14 days, and **c** exposed to 15 wt% sulfuric acid solution for 14 days

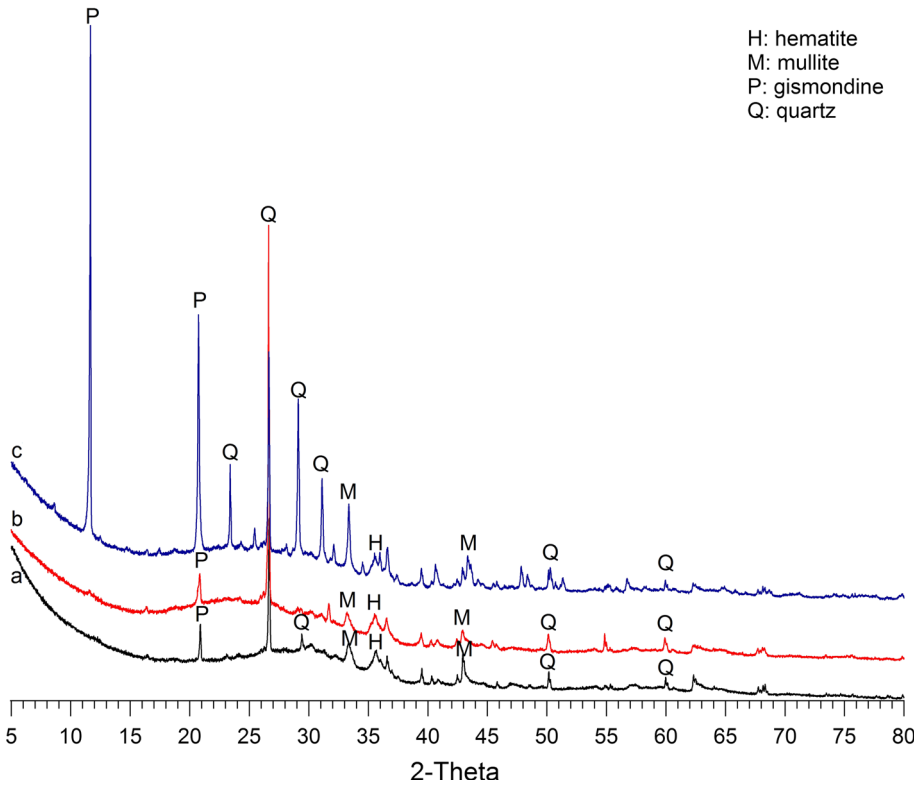

Fig. 10 XRD of NG3 samples **a** before test, **b** exposed to 15 wt% hydrochloric acid solution for 14 days, and **c** exposed to 15 wt% sulfuric acid solution for 14 days

enhancing the hydration of the cement as the sharper peaks represented a high activation energy. It is also interesting to note that a large activation energy was also involved when the samples were exposed to the acidic environment. No significant change was detected after the sample was exposed to hydrochloric acid, but not with sulfuric acid. Similar to Fig. 7, there were some new additional peaks which corresponded to gismondine and quartz minerals after the sample was tested in sulfuric acid environment.

Figure 9 shows the effect of adding 2 wt. % Nano-silica to the cement system. Before the test, the peak representing quartz at 27° has the same intensity as in Fig. 8, but it is not detected at 29°. The significant difference seen in Fig. 9 was the behavior of the cement sample when exposed to hydrochloric acid. The stronger peaks that were detected after hydrochloric acid attack indicated that the aluminosilicate structure in the before-test geopolymer could have been destroyed which required large activation energy for this purpose. This behavior had explained the result obtained in Fig. 1 which showed that the compressive strength of NG2_H was lower than NG2_S, while the diffraction peak behavior of the sample being exposed to sulfuric acid also showed the same behavior as GC_S and NG1_S in Figs. 7 and 8, respectively.

The effect of adding 3 wt. % Nano-silica in the geopolymer cement system is shown in Fig. 10. The profile for this sample is quite similar with that in Figs. 7, 8 and 9. The differences can be seen by minutely examining the profile. Before the test, the peak at angle 27°, which represents quartz mineral, was sharper than the profile in Fig. 7, while the quartz diffraction peak was also detected at angle 29°, which is not detected in Fig. 9. This behavior had explained the higher compressive strength of NG3_B as compared with NG2_B. After being exposed to hydrochloric acid environment, the peak which corresponded to quartz as sharply detected at angle 27°, but the intensity was lower than the sample in Fig. 9, while after being tested in sulfuric acid, the profile was quite similar to other geopolymer samples exposed in the same environment, only that the sample in Fig. 10 had a lower intensity.

Based on the XRD analysis above, it is deduced that the XRD profiles for all geopolymer samples with and without Nano-silica showed a similar behavior before and after acid exposure with the intensity being the only difference. In comparison with the peak before acid exposure, the stronger and sharper peak in the samples after acid attack indicated that the aluminosilicate structure could have been destroyed and formed a different type of amorphous structure. Other hydration products were not apparent in XRD results due to the crystal surface being covered by amorphous phases formed, thereby blocking the XRD reflections that would have otherwise been generated by these minerals. When comparing all XRD results of geopolymer cement samples, the minerals found in all samples were still detected after acid exposure. Geopolymer cement samples exposed to sulfuric acid exhibited additional peaks, which represented gismondine and quartz.

XRD pattern of the OPC samples before and after the test is shown in Fig. 11. OPC samples showed significant changes in the diffraction pattern after 14 days of 15 wt. % hydrochloric acid and sulfuric acid exposure due to the formation of gypsum and ettringite which subsequently led to the expansion and spalling of surface layers. Before acid exposure, the peaks representing portlandite (calcium hydroxide) were easily distinguished in the regions of 18°, 32°, 47° and 51°, while the C–S–H peaks were detected at 28°, 34° and 54°. However, ettringite and gypsum were also detected before the test, but their intensity was quite low. After acid exposure, portlandite (P) which could readily be identified in the XRD results of OPC cement was absent at the angle of 18° but was detected at 32° for both OPC_H and OPC_S and 48° and 51° for OPC_S. Meanwhile, the peaks representing C–S–H gel were also detected after the test which indicated that OPC can still withstand an acidic environment. However, ettringite and gypsum peaks were sharply detected after the test as indicated by the peak at the angle of 12° and 21°, respectively, which caused them to suffer strength reduction.

3.3 Microstructure Behavior of Class G and Geopolymer Cement

3.3.1 SEM

SEM micrographs, as shown in Figs. 12, 13, 14, 15 and 16, provided qualitative representation about reaction efficiency of geopolymer and Class G cement. The microstructure figures were obtained by using transmitted light microscopy on thin sections of the cement samples at 1500× magnification. SEM image for pure geopolymer cement is shown in Fig. 12. Unreacted fly ash was in sphere-shaped form, while reactive geopolymer cement was uneven with irregular shape. Before acid exposure, GC_B in Fig. 12a showed a fair amount of unreacted fly ash. The presence in concave-circular shaped were detected in Fig. 12a. These shapes indicated there was an oxidation process occurred, a substantially fast chemical reaction, which resulted in three-dimensional polymeric chain and ring structure consisting of Si–O–Al–O bonds called polymerization process. This process was also confirmed by [5,8], which contributed to the increase in strength of the cement sample, while GC_H and GC_S shown in Fig. 12b, c showed a fair homogeneous matrix with most of fly ash particles disappeared after being exposed into 15 wt% hydrochloric acid and sulfuric acid solutions for 14 days. However, major cracks were observed after GC samples were exposed into acidic environment. It indicated that acid had penetrated through GC cement samples, thus reacted with minerals and caused them to lose strength, as shown in Fig. 1.

Typical microstructure of geopolymer cement with 1 wt.%, 2 wt% and 3 wt% addition of Nano-silica before acid exposure is shown in Figs. 13a, 14a and 15a, respectively. SEM image of NG1_B in Fig. 13a was quite different as compared to other geopolymer cement samples before acid exposure, where it has denser and compact microstructure. Instead of filling up the voids, increasing Nano-silica concentration to 2 and 3 wt% created more voids. These significant changes in the microstructure of the geopolymer cement with the addition of 1 wt.% Nano-silica explained the significant changes in its physical and chemical characteristics. The existence of more voids when increasing Nano-silica concentration may be due insufficient hydration, thus decreasing geopolymerization and pozzolanic reaction rate which then led to the lower compressive strength. NG1 samples had higher compressive strength value, mainly because the voids were lesser causing the acid solutions not be able to fully penetrate the cement system and react with the chemical substances in the cement samples. Besides, the presence in concave-circular shape for NG1 were more than other geopolymer samples. It proved the workability of Nano-silica, which accelerated the oxidation process and at the same time increased its strength.

The microstructure behavior of the geopolymer cement with Nano-silica admixture exposed to the acidic environment is shown in Figs. 13b, c, 14b, c and 15b, c. Similar to pure geopolymer cement sample, micrographic changes were obvious after the geopolymer cement with Nano-silica admixture was treated with 15 wt% hydrochloric and 15 wt% sulfuric acid solutions. They suffered crack after acid exposure. Figure 13b shows that acid managed to dissolve the minerals in the cement system and increased its porosity, while Fig. 13c shows that the unreacted fly ash particles in Fig. 13a had changed its form and major cracks can be observed. The surface was covered with reaction products because they are different from the substances observed in Fig. 13a. Next, Fig. 14b, c shows the effect of acid solution toward 2 wt.% incorporated Nano-silica in geopolymer cement system. After being exposed to 15 wt.% hydrochloric acid, NG2_H sample in Fig. 14b shows that there was the presence of slightly long-bar-shaped as if they had undergone crystallization and suffered strength degradation because of the crack observed, while NG2_S sample in Fig. 14c shows that the unreacted fly ash in Fig. 14a had reacted with sulfuric acid and caused it to suffer crack. Next, it is interesting to note the microstructure image of geopolymer cement with 3 wt.% addition of Nano-silica in Fig. 15a. It is quite different with other unexposed geopolymer cement samples where the surface was covered with reaction product but after the test, it had disappeared. It indicated that the reaction product had reacted with acid and caused it to dissolve. After the test, both NG3_H and NG3_S samples in Fig. 15b, c had also suffered crack and became more porous.

However, it must be acknowledged that although all the geopolymer cement samples, with and without Nano-silica, suffered crack after being tested in the 15 wt% hydrochlo-

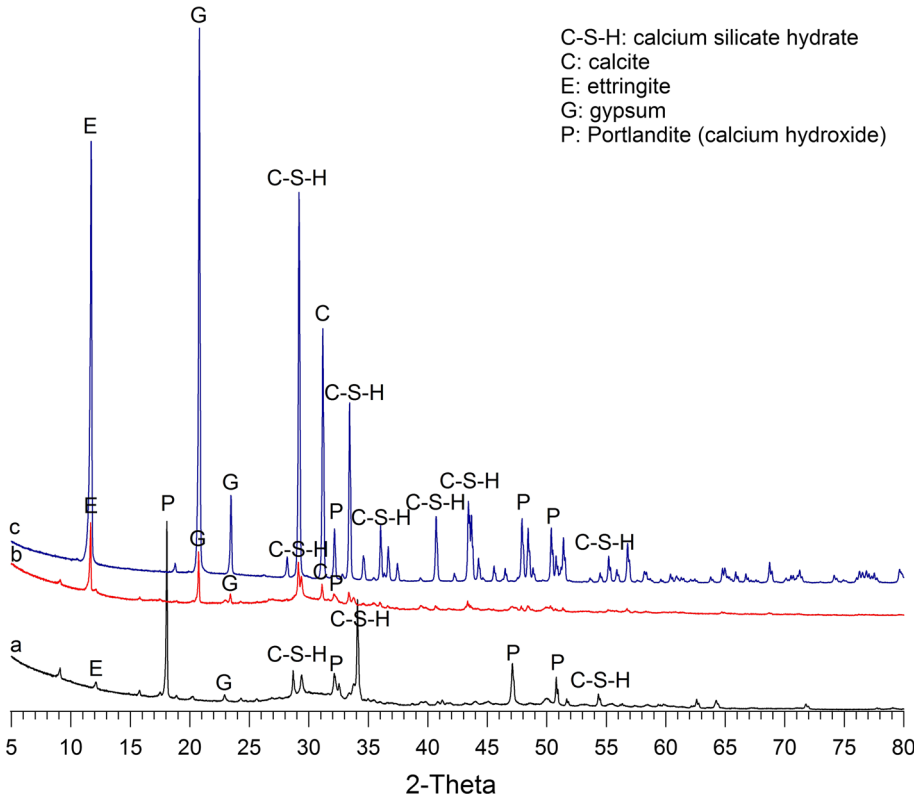

Fig. 11 XRD of OPC samples **a** before test, **b** exposed to 15 wt% hydrochloric acid solution for 14 days, and **c** exposed to 15 wt% sulfuric acid solution for 14 days

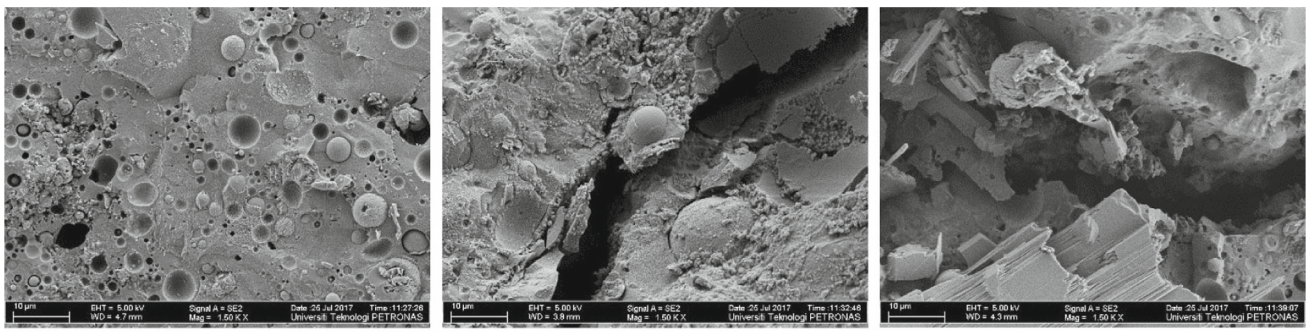

(a) **(b)** **(c)**

Fig. 12 Microstructure observation of GC samples before and after the test. **a** Before test, **b** exposed to 15 wt% hydrochloric acid solution for 14 days, **c** Exposed to 15 wt% sulfuric acid solution for 14 days

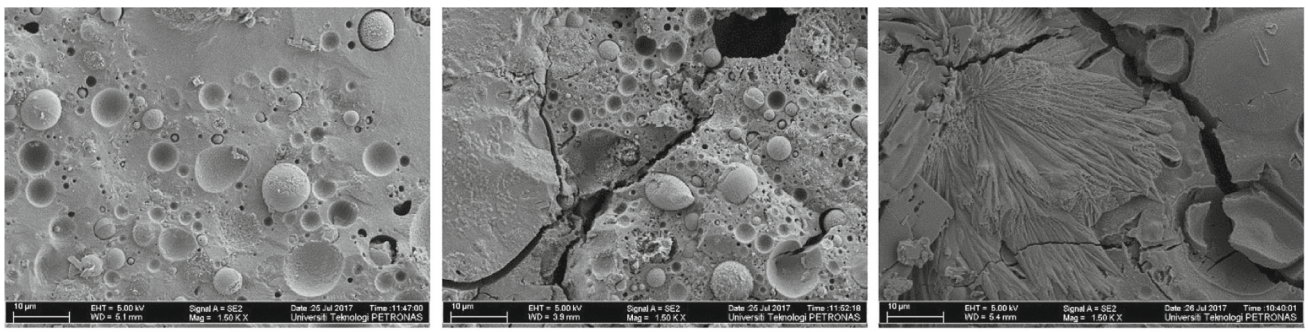

(a) **(b)** **(c)**

Fig. 13 Microstructure observation of NG1 samples before and after the test. **a** Before test, **b** exposed to 15 wt% hydrochloric acid solution for 14 days, **c** Exposed to 15 wt% sulfuric acid solution for 14 days

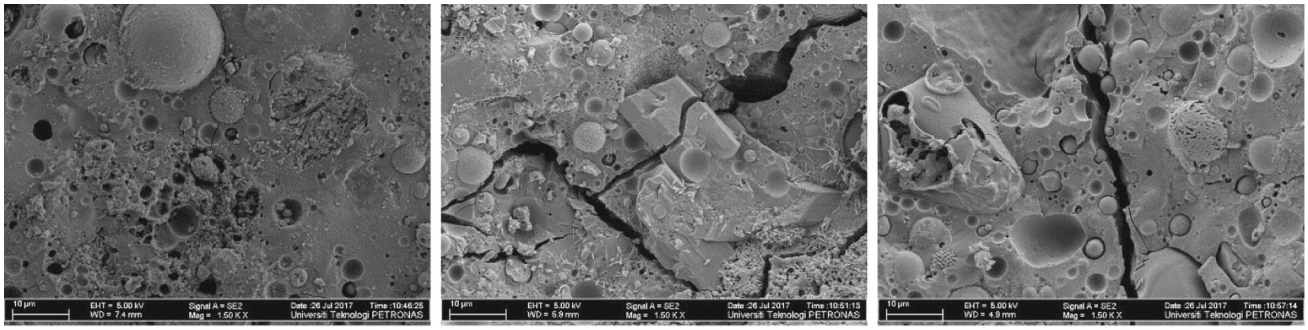

(a) (b) (c)

Fig. 14 Microstructure observation of NG2 samples before and after the test. **a** Before test, **b** exposed to 15 wt% hydrochloric acid solution for 14 days, **c** Exposed to 15 wt% sulfuric acid solution for 14 days

(a) (b) (c)

Fig. 15 Microstructure observation of NG3 samples before and after the test. **a** Before test, **b** exposed to 15 wt% hydrochloric acid solution for 14 days, **c** Exposed to 15 wt% sulfuric acid solution for 14 days

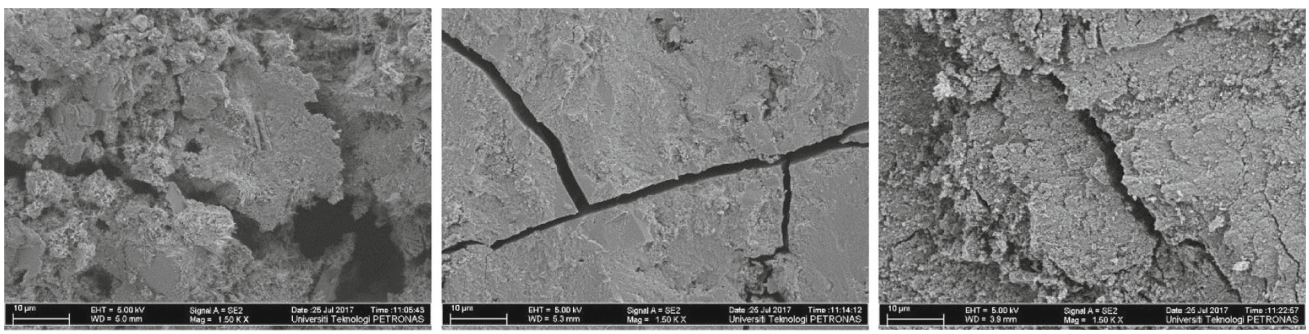

(a) (b) (c)

Fig. 16 Microstructure observation of OPC samples before and after the test. **a** Before test, **b** exposed to 15 wt% hydrochloric acid solution for 14 days, **c** Exposed to 15 wt% sulfuric acid solution for 14 days

ric acid and 15 wt% sulfuric acid for 14 days, the fly ash spheres and other minerals remained and were not completely dissolved. Thus, this behavior had explained the strength obtained by these samples which are still higher as compared with Class G cement as shown in Fig. 1.

SEM image for Class G controlled samples, OPC_B, is shown in Fig. 16. It can be observed that OPC_B (Fig. 16a) suffered damage even before exposing it to acid solutions. This structure was observed due to the high curing condition that had broken up the intergranular structure of the cement, thus decreasing its strength. Figure 16b, c shows SEM images for OPC_H and OPC_S, respectively. After acidic exposure, most of OPC minerals was observed to have reacted with the acid solutions. Hydrochloric and sulfuric acids managed to penetrate OPC cement sample and caused them to degrade and form major cracks. The OPC samples reacted aggressively, thus explaining the lower compressive strength value.

3.3.2 EDS Analysis

Figure 17 shows the EDS result of geopolymer and Class G cement before and after being exposed to the acidic environment. Before being exposed to the acidic environment, GC_B showed a fair amount of sodium, silica and aluminum contents. After the test, the amount of Na and Al decreased for both GC_H and GC_S, while Si ions were increased for GC_H sample. It indicated that although the cement samples were affected by acid, they still gained strength since sodium ions were part of N-A-S-H gel. As compared to both after treatment samples, it was obvious that pure geopolymer cement sample was affected more in 15 wt% sulfuric acid as the amount of sodium, aluminum and silica ions was lower than the sample exposed with 15 wt% hydrochloric acid.

Interestingly, the amount of silica in all geopolymer cement with Nano-silica admixture before the test was higher than GC_B sample. The amount of silica in NG1_B, NG2_B and NG3_B also increased with the increasing amount of Nano-silica which was reported as 17.46, 20.68 and 22.36 wt%, respectively. This indicated that the workability of Nano-silica as a filler effects to fill up the empty spaces, thus increasing the amount of silica content inside the cement matrix. Meanwhile, the amount of sodium content was decreased with increasing amount of Nano-silica. After exposed to acid solutions, NG1 sample proved that it can withstand an acid environment as the presence of chloride ions in NG1_H and sulfur ions in NG1_S is the lowest as compared to the other geopolymer cement samples. It indicated that hydrochloric acid and sulfuric acid used in this research were not able to fully penetrate the NG1 samples. The presence of chloride ions and sulfur ions in the NG1_H and NG1_S samples was 2.99 and 0.38 wt%, respectively, while NG2 sample showed that there was a presence of 3.80 wt% of chloride ions and 0.78 wt% of sulfur ions in the sample. It can also be seen the presence of chloride ions in the NG3_H sample was 3.69 and 2.61 wt% of sulfur ions in NG3_S sample.

Next, the calcium ions in OPC_B was quite high, which was 34.38 wt% as can be seen in Fig. 17. After the test, calcium ions were decreased. Hydrochloric and sulfuric acids had reacted with the minerals in OPC samples. The amount of chloride ions in OPC_H and sulfur ions in OPC_S was 1.95 and 1.42 wt%, respectively. Although the amount of acids that manage to penetrate OPC sample was quite low, it had severely affected the sample. This finding is agreed with [4]. The gypsum was generated when calcium hydroxide reacted with sulfuric acid, which was the main degradation product of OPC samples. In this study, calcium ions in OPC were consumed by acid to form gypsum ($CaSO_4$) and ettringite ($(Ca_6Al_2(SO_4)_3(OH)_{12}\cdot 26H_2O)$, in which their presence was reported in FTIR and XRD data in Figs. 5 and 10, respectively.

From the EDS results obtained, these findings were in agreement with FTIR and XRD data obtained in the previous section. It can be deduced that hydrochloric and sulfuric acids had managed to penetrate the geopolymer and Class G cement. The acid solutions had reacted with the minerals inside the cement system and thus had led to strength degradation. However, the severity of the dam-

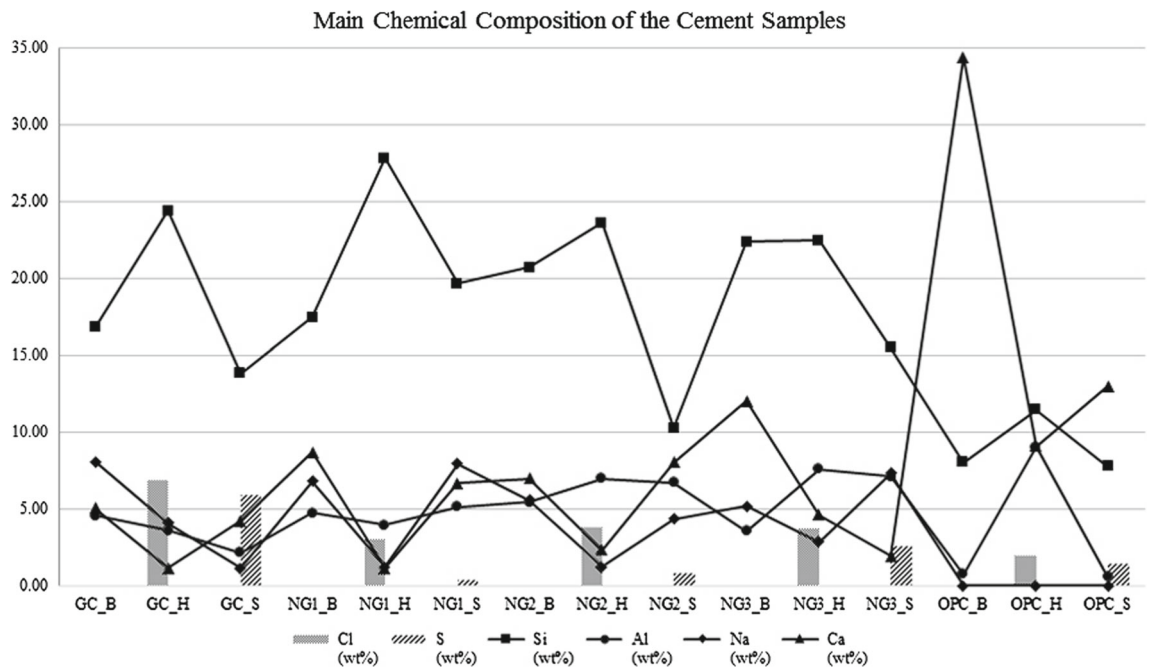

Fig. 17 EDS result of the cement samples before and after exposed to acidic environment

age for geopolymer cement samples was not threatening as the compressive strength for each of the samples that were reported in Fig. 1 was still higher than Class G cement. All geopolymer cement samples showed the presence of N-A-S-H gel and gismondine ($CaAl_2SiO_8.4H_2O$) in FTIR and XRD data, respectively, which indicated that all geopolymer cement samples gained in strength and managed to hydrate, only that it is fully effective with a low amount of Nano-silica content.

4 Conclusion

The fundamental structure of materials can be altered by using nanotechnology to enhance its performance and properties. Based on the present experimental study, it is concluded that:

1. The enhanced Nano-silica cement had the best resistance in acidic environment for oil well with 65°C temperature. The inclusion of 1 wt.% Nano-silica into geopolymer cement caused an increase in strength based on compressive strength, FTIR and XRD results obtained.
2. Compressive strength results showed that NG1 had the highest strength before and after the test, while OPC samples were the lowest.
3. FTIR results for all geopolymer cements before acid exposure indicated that all cement samples had gained strength as the geopolymerization has taken place at 960 cm^{-1} regions where Si/Al ratio was increased and the main binder gel for geopolymer cement, N-A-S-H gel, was formed. However, geopolymer cements, with and without Nano-silica, suffered depolymerization after acid exposure as they shifted to a higher frequency region, thus affecting their structure and influencing the compressive strength result.
4. XRD analysis showed that the strength of all geopolymer samples was increased because of the presence of gismondine, a hydrated aluminosilicate mineral in the cement system, while OPC samples were degraded in strength due to the presence of ettringite and gypsum.
5. SEM images of NG1 samples proved the workability of Nano-silica in filling up the empty spaces as its microstructure was denser and compact as compared to GC, NG2 and NG3. This compact surface had managed to prevent the acid solutions from fully penetrating the cement system.
6. EDS result had shown the Nano-silica workability because the amount of silica in geopolymer cement with Nano-silica additive was increased. After being exposed to acid solutions, NG1 again proved that it was superior to other samples in acidic environment as the amount of chloride and sulfur present in the cement system after the test was low.

The stability of geopolymer cement in acidic environment depended on the amount of Nano-silica that was included in the recipe, and it had worked as expected in the literature. Nano-silica had managed to aid and enhance the geopolymer cement performance inside the oil well at 65 °C.

Acknowledgements The authors wish to express their gratitude to Universiti Teknologi PETRONAS for providing laboratory facilities and research fund under the Fundamental Research Grant Scheme (FRGS) Project No. 0153AB-K96.

References

1. Agapiou, K.; Charpiot, S.: Cement and wellbore integrity. Int. Cem. Rev.: Oilw. Cem., 113-116 (2013)
2. Choi, Y.S.; Young, D.; Nesic, S.; Gray, L.G.S.: Wellbore integrity and corrosion of carbon steel in CO_2 geologic storage environment: a literature review. Int. J. Greenh. Gas Control **16**, S70–S77 (2013)
3. Nasvi, C.M.; Ranjith, P.G.; Sanjavan, J.: Geopolymer as well cement and variation of its mechanical properties under different curing temperature and curing mediums. Greenh. Gases Sci. Technol. **2**(1), 46–58 (2012)
4. Izzat, A.M.; Abdullah, M.; Hussin, K.; Sandu, A.V.; Ghazali, C.M.R.; Mohd Tahir, M.F.; Ligia, M.M.: Sulfuric acid attack on ordinary portland cement and geopolymer material. Rev. Chim. (Bucharest) **64**(9), 1011–1014 (2013)
5. Bensted, J.: Class G and H basic oilwell cements. World Cem., pp 44–50 (1992).
6. Ryu, G.S.; Lee, Y.B.; Koh, K.T.; Chung, Y.S.: The mechanical properties of fly ash-based geopolymer concrete with alkaline activators. Constr. Build. Mater. **47**, 409–418 (2013)
7. Adak, D.; Sarkar, M.; Mandal, S.: Effect of nano-silica on strength and durability of fly ash based geopolymer mortar. Constr. Build. Mater. **70**, 453–459 (2014)
8. Maheswaran, S.: Study on effect of low calcium fly ash on geopolymer cement for oil well cementing. In: Paper SPE 176454 Presented at the SPE/IATMI Asia Pacific Oil & Gas Conference and Exhibition, Nusa Dua, Bali, Indonesia, 20–22 October (2015). https://doi.org/10.2118/176454-MS.
9. Mahmoudkhani, A.H.; Huynh, D.; Sylvestre, C.J.; Schneider, J.: New environment- friendly cement slurries with enhanced mechanical properties for gas well cementing. In: Paper SPE 115004 Presented at the CIPC/SPE Gas Technology Symposium 2008 Joint Conference, Calgary, Alberta, Canada, 16–19 (2008). https://doi.org/10.2118/115004-MS.
10. Bakharev, T.: Geopolymeric materials prepared using class F fly ash and elevated temperature curing. Cem. Concr. Res. **35**(6), 1224–1232 (2005)
11. Srivinasan, K.; Sivakumar, A.: Geopolymer binders: a need for future concrete construction. ISRN Polymer Sci. 2013, Article ID 509185 (2013). https://doi.org/10.1155/2013/509185.
12. Ridha, S.; Yerikania, U.: New nano-geopolymer cement system improves wellbore integrity upon acidizing job: Experimental findings. In: Paper SPE 176419 Presented at the SPE/IATMI Asia Pacific Oil & Gas Conference and Exhibition, Nusa Dua, Bali, Indonesia, 20–22 October (2015). https://doi.org/10.2118/176419-MS.
13. Davidovits, J.: Properties of geopolymer cement. Alkaline Cem. Concr., 131–149 (1994)

14. Salehi. S.; Khattak, M.J.; Ali, N.; Rizvi, H.R.: Development of geopolymer-based cement slurries with enhanced thickening time, compressive and shear bond strength and durability. In: Paper SPE 178793 Presented at the IADC/SPE Drilling Conference and Exhibition, Fort Worth, Texas,USA, 1–3 March (2016). https://doi.org/10.2118/178793-MS.
15. Hewayde, E.; Nehdi, M.; Allouche, E.; Nakhla, G.: Effect of geopolymer cement on microstructure, compressive strength and sulfuric acid resistance of concrete. Mag. Concr. Res. **58**(5), 321–33 (2006)
16. Santra, A.; Boul, P.J.; Pang, X.: Influence of nanomaterials in oilwell cement hydration and mechanical properties. In: Paper SPE 156937 Presented at the SPE International Oilfield Nanotechnology Conference, Noorwijk, The Netherlands, 12–14 June (2012). https://doi.org/10.2118/156937-MS.
17. Duxson, P.; Fernández-Jiménez, A.; Provis, J.L.; Lukey, G.C.; Palomo, A.; van Deventer, J.S.J.: Geopolymer technology: the current state of the art. J. Mater. Sci. **42**(9), 2917–2933 (2007)
18. Davidovits, J.: Geopolymer Chemistry and Applications, 3rd edn. Institute Geopolymer, Saint-Quentin (2011)
19. Houseworth, J.: Advanced Well Stimulation Technologies in California Chapter 2, p. 61. CCST Publication, Sacramento (2016)
20. Stegent, N.A.; Wagner, A.L.; Mullen, J.; Borstmayer, R.E.: Engineering a successful fracture-stimulation treatment in the eagle ford shale. In: Paper SPE 136183 Presented at the SPE Tight Gas Completions Conference, San Antonio, Texas, USA, 2–3 November 2010. https://doi.org/10.2118/136183-MS.
21. A. C 109/C 109M – 07: Standard test method for compressive strength of hydraulic cement mortars (using 2-in. or [50-mm] cube specimens). ASTM International (2008)
22. Syed, T.: EPA Hydraulic Fracturing Workshop, 2011. Retrieved December 22, 2017, from https://www.epa.gov/sites/production/files/documents/cementingandzonalisolationforhfwells.pdf
23. Bakharev, T.: Resistance of geopolymer materials to acid attack. Cem. Concr. Res. **35**, 658–670 (2005)
24. Hughes, T.L.; Methven, C.M.; Jones, T.G.J.; Pelham, S.E.; Fletcher, P.; Hall, C.: Determining cement composition by Fourier Transform Infrared Spectroscopy. Adv. Cem. Based Mater. **2**, 91–104 (1995)